

Stimulated scattering instability in a relativistic plasma

A. P. Misra^{1,*} and Debjani Chatterjee^{1,†}

¹*Department of Mathematics, Siksha Bhavana, Visva-Bharati University, Santiniketan-731 235, West Bengal, India*

We study the stimulated scattering instabilities of an intense circularly polarized electromagnetic (CPEM) wave in a degenerate relativistic electron-ion plasma. Starting from a relativistic hydrodynamic model and the Maxwell's equations, we derive coupled nonlinear equations for low-frequency electron and ion plasma oscillations that are driven by the CPEM ponderomotive force. The nonlinear dispersion relations are then obtained from the coupled nonlinear equations which reveal stimulated Raman scattering (SRS), stimulated Brillouin scattering (SBS), and modulational instabilities (MIs) of CPEM waves. It is shown that the thermal pressure of ions and the relativistic degenerate pressure of electrons significantly modify the characteristics of SRS, SBS, and MIs.

PACS numbers: 52.25.Dg, 52.27.Ep, 52.35.Mw, 52.35.Sb

I. INTRODUCTION

The nonlinear self-interactions of large amplitude intense electromagnetic (EM) waves and relativistic/nonrelativistic plasmas have received a significant research attention in recent years (see, e.g., Refs. 1–10). Such high-frequency (hf) EM waves are used for plasma heating, e.g., in inertial fusion plasmas [11], as well as for plasma diagnostics [12], e.g., in solid density plasmas that are created by intense laser and charged particle beams. Furthermore, laser-plasma interaction provides a rich source of nonlinear phenomena including the formation of coherent structures as localized bursts of x rays and γ rays [13] from compact astrophysical objects, fast ignition, particle acceleration, generation of different kinds of waves and instabilities [14]. So, under certain conditions, the collective parametric effects such as stimulated Raman and Brillouin scattering instabilities, and localization of high-frequency (hf) EM waves could have a definite signature on the radiation spectra (ranging from radio to γ rays) of astrophysical objects [15]. On the other hand, for high-density plasmas, such as those in the interior of white dwarfs, neutron stars, and also at the source of γ -ray bursts [16], the relevant plasmas are relativistically degenerate and thus obey the Fermi-Dirac statistics.

In a recent study, it has been shown that the stimulated Raman scattering instability is influenced by the weak and strong degeneracy of electrons in relativistic plasmas [1]. In another work, it has been emphasized that not only the Raman and Brillouin scattering instabilities are possible, there can be the onset of modulational instabilities of the circularly polarized electromagnetic (CPEM) waves at nanoscales in dense quantum plasmas [2].

In this work, we present a theoretical study on the stimulated scattering instabilities of intense hf CPEM waves in a relativistic plasma with degenerate electrons

and adiabatic thermal ions. Starting from the CPEM wave equation coupled to the driven (by the CPEM ponderomotive force) equations for low-frequency electron and ion plasma oscillations, we obtain nonlinear dispersion relations that reveal stimulated Raman scattering (SRS), stimulated Brillouin scattering (SBS) and modulational instabilities (MIs) of CPEM waves. It is shown that in the field of strong EM radiation, the instabilities develop and the corresponding growth rates become high in weakly relativistic degenerate plasmas with thermal ions.

II. THEORETICAL FORMULATION

We consider the nonlinear interactions of intense CPEM waves and the relativistic plasma composed of degenerate electrons and adiabatic thermal ions. The propagation of CPEM waves is governed by the following equation [2, 17]

$$\left(\frac{\partial^2}{\partial t^2} - c^2 \nabla^2 + \omega_p^2\right) \mathbf{A} + \frac{\omega_p^2}{n_0} \left(\frac{n_e}{\gamma_e} + m \frac{n_i}{\gamma_i}\right) \mathbf{A} = 0, \quad (1)$$

which is derived from the Ampere-Maxwell equation, given by,

$$\nabla \times \mathbf{B} = \frac{1}{c} \left(4\pi c \mathbf{J} + \frac{\partial \mathbf{E}}{\partial t}\right), \quad (2)$$

plus the equations of motion for electrons and ions together with the scalar and vector potentials, defined by,

$$\mathbf{B} = \nabla \times \mathbf{A}, \quad \mathbf{E} = -\frac{1}{c} \frac{\partial \mathbf{A}}{\partial t} - \nabla \phi, \quad (3)$$

and the coulomb's gauge condition $\nabla \cdot \mathbf{A} = 0$.

In Eq.(1), c is the speed of light in vacuum, $\omega_p = \sqrt{4\pi n_0 e^2 / m_e}$ is the electron plasma oscillation frequency, n_0 is the background number density of electrons/ions, $m = m_e / m_i$ is the ratio of electron to ion masses in rest frame and n_e (n_i) is the electron (ion) number density.

* apmisra@visva-bharati.ac.in; apmisra@gmail.com

† chatterjee.debjani10@gmail.com

Furthermore, γ_e and γ_i , respectively, denote the relativistic factors for electrons and ions, given by,

$$\gamma_e = \sqrt{\frac{1 + |\mathbf{A}|^2}{1 - v_e^2}}, \quad \gamma_i = \sqrt{\frac{1 + m^2 |\mathbf{A}|^2}{1 - v_i^2}}. \quad (4)$$

In Eq. (1), we have retained the relativistic effects for both electrons and ions for the sake of completeness, and also to the fact that the laser amplitude may be high enough to drive ions with relativistic velocities.

The governing equations for low-frequency electron and ion plasma oscillations driven by the CPEM ponderomotive force are

$$\frac{\partial n_j}{\partial t} + \nabla \cdot (n_j \mathbf{v}_j) = 0, \quad (5)$$

$$\left(\frac{\partial}{\partial t} + \mathbf{v}_j \cdot \nabla \right) (\gamma_j \mathbf{v}_j) = -\frac{q_j}{m_j} \nabla (\phi + \phi_{pj}) - \frac{1}{m_j n_j} \nabla P_j, \quad (6)$$

$$\nabla^2 \phi = 4\pi e (n_e - n_i), \quad (7)$$

where \mathbf{v}_j is the fluid velocity, $\phi_{pj} = q_j |\mathbf{A}|^2 / m_j c^2$ is the ponderomotive potential associated with the CPEM waves [17], P_j is the fluid pressure, q_j is the charge of the j -th species particle ($j = e$ for electrons and i for ions), and ϕ is the electrostatic potential. For simplicity, we assume that the CPEM waves propagate in the x -direction, i.e., all the dynamical variables vary with x and t , and $\mathbf{A} = (\mathbf{A}_\perp, 0)$.

Next, normalizing the variables according to $n_j \rightarrow n_j/n_0$, $v_j \rightarrow v_j/c$, $x \rightarrow x\omega_p/c$, $t \rightarrow t\omega_p$, $\phi, \mathbf{A} \rightarrow e(\phi, \mathbf{A})/m_e c^2$, we recast Eqs. (1), (5)-(7) as

$$\left(\frac{\partial^2}{\partial t^2} - \frac{\partial^2}{\partial x^2} + 1 \right) \mathbf{A}_\perp + \left(\frac{n_e}{\gamma_e} + m \frac{n_i}{\gamma_i} \right) \mathbf{A}_\perp = 0, \quad (8)$$

$$\frac{\partial n_e}{\partial t} + \frac{\partial}{\partial x} (n_e v_e) = 0, \quad (9)$$

$$\left(\frac{\partial}{\partial t} + v_e \frac{\partial}{\partial x} \right) (\gamma_e v_e) = \frac{\partial}{\partial x} \left(\phi - \frac{|\mathbf{A}_\perp|^2}{2\gamma_e} \right) - \frac{\sigma_e}{n_e} \frac{\partial n_e}{\partial x}, \quad (10)$$

$$\frac{\partial n_i}{\partial t} + \frac{\partial}{\partial x} (n_i v_i) = 0, \quad (11)$$

$$\left(\frac{\partial}{\partial t} + v_i \frac{\partial}{\partial x} \right) (\gamma_i v_i) = -m \frac{\partial}{\partial x} \left(\phi + \frac{m |\mathbf{A}_\perp|^2}{2\gamma_i} \right) - \frac{\sigma_i}{n_i} \frac{\partial n_i}{\partial x}, \quad (12)$$

$$\frac{\partial^2 \phi}{\partial x^2} = n_e - n_i, \quad (13)$$

where the term $\propto \sigma_e = (2/3)\mathcal{E}_F/\alpha_0 m_e c^2$ appears due to the degeneracy pressure of electrons P_e , given by [18],

$$\begin{aligned} P_e &= P_{e0} + \left(\frac{\partial P_e}{\partial n_e} \right)_{n_e=n_0} n_{e1} + \frac{1}{2} \left(\frac{\partial^2 P_e}{\partial n_e^2} \right)_{n_e=n_0} n_{e1}^2 + \dots, \\ &= P_{e0} + \frac{2}{3\alpha_0} \mathcal{E}_F n_{e1} + \frac{R^2 + 2}{9\alpha_0^3 n_0} \mathcal{E}_F n_{e1}^2 + \dots, \end{aligned} \quad (14)$$

where $\alpha_0 = \sqrt{1 + R^2}$, $R = p_0/m_e c$ is the dimensionless parameter which measures the strength of the plasma degeneracy, $p_0 = (3\hbar^3 n_0/8\pi)^{1/3}$ is the momentum of electrons on the Fermi surface, and $\mathcal{E}_F = \hbar^2 (3\pi n_0)^{2/3}/2m_e$ is the Fermi energy. The case with $R \ll 1$ ($\gg 1$) corresponds to the weakly relativistic (ultra-relativistic) degenerate plasmas. In Eq. (10), the higher order terms involving the perturbed number density n_{e1} in the pressure gradient term are not considered as those will not contribute to the corresponding linear terms. Also, the ion fluid pressure is given by $P_i = \Gamma_i k_B T_i$ with Γ_i denoting the adiabatic factor.

In what follows, we derive the governing equations for the low-frequency electron and ion plasma oscillations that are driven by the CPEM ponderomotive force in a relativistic degenerate plasma. First, we consider the stimulated Raman scattering of CPEM waves associated with the driven electron plasma oscillations on the time scale of electron plasma period ω_p^{-1} . In this case, ions can be considered as immobile for which the ion density perturbation is zero. Thus, linearizing Eqs. (8), (9), and (13), we obtain

$$\left(\frac{\partial^2}{\partial t^2} - \frac{\partial^2}{\partial x^2} + 1 \right) \mathbf{A}_\perp + \frac{N_e \mathbf{A}_\perp}{\gamma_{e0}} = 0, \quad (15)$$

$$\left(\frac{\partial^2}{\partial t^2} - \sigma_e \frac{\partial^2}{\partial x^2} + \frac{1}{\gamma_{e0}} \right) N_e = \frac{1}{2\gamma_{e0}^2} \frac{\partial^2}{\partial x^2} |\mathbf{A}_\perp|^2, \quad (16)$$

where $\gamma_{e0} = \sqrt{1 + A_0^2}$ with A_0 denoting the amplitude of the CPEM pump and $N_e = n_{e1}/n_0 \ll 1$.

Second, we consider the stimulated Brillouin scattering associated with the low-frequency ion plasma oscillations. In this case, we assume that $|\partial^2 N_e / \partial t^2| \ll |\sigma_e \partial^2 N_e / \partial x^2|$ for which one can neglect the left-hand side of Eq. (10), and make use of the reduced equation to eliminate $\partial\phi/\partial x$ from Eq. (12). Thus, linearizing Eqs. (11) and (12) and assuming the quasineutrality $n_{e1} \approx n_{i1}$ (valid for long-wavelength low-frequency perturbations), we obtain the following wave equation for the driven ion plasma oscillations.

$$\left(\frac{\partial^2}{\partial t^2} - \sigma \frac{\partial^2}{\partial x^2} \right) N_e = \frac{\beta}{2} \frac{\partial^2}{\partial x^2} |\mathbf{A}_\perp|^2, \quad (17)$$

where $\sigma = (m\sigma_e + \sigma_i)/\gamma_{i0}$, $\beta = m(1 + m\gamma_{e0})/\gamma_{e0}\gamma_{i0}$, $\sigma_i = \Gamma_i k_B T_i/m_e c^2$ and $\gamma_{i0} = \sqrt{1 + m^2 A_0^2}$. Equations (15) to (17) are the desired equations describing the onset of stimulated scattering instabilities and localization of EM solitons in relativistic plasmas with degenerate electrons and adiabatic thermal ions.

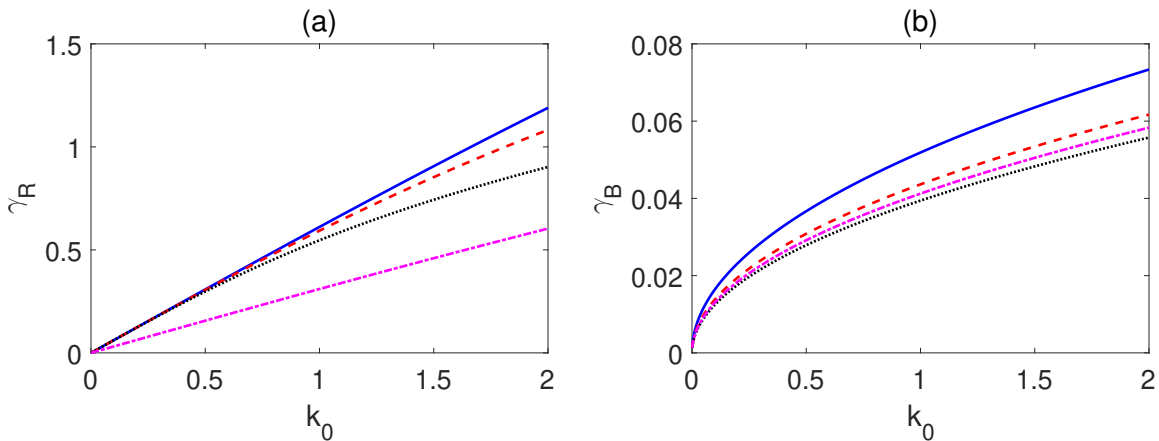


FIG. 1. The growth rates are shown for the stimulated Raman scattering (γ_R) and stimulated Brillouin scattering (γ_B) instabilities [Eq. (23)]. In the subplot (a), the solid, dashed and dotted lines are corresponding to the number densities $n_0 = 10^{28} \text{ cm}^{-3}$, 10^{29} cm^{-3} and 10^{30} cm^{-3} for which $\sigma_e = 0.01$, $R = 0.2$, $\sigma_e = 0.04$, $R = 0.46$ and $\sigma_e = 0.16$, $R = 1.0$ respectively, and with a fixed value of $A_0 = 1.3$. The dash-dotted line is for a higher value of $A_0 = 10$ with a fixed $n_0 = 10^{28} \text{ cm}^{-3}$. In the subplot (b), the solid, dashed and dotted lines are corresponding to $\sigma_i = 0.01$, 0.02 and 0.03 respectively, and with a fixed $A_0 = 10$. The dash-dotted line is for a lower value of $A_0 = 1.3$ with a fixed $n_0 = 10^{28} \text{ cm}^{-3}$. The other parameter values are as for the solid line in the subplot (a).

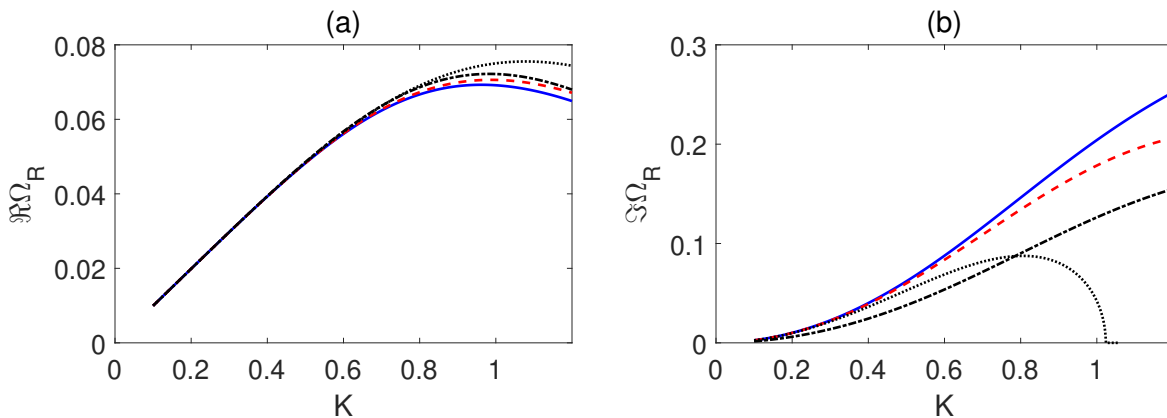


FIG. 2. The frequency shift ($\Re\Omega$) and the growth rate of instability ($\Im\Omega$) [numerical solutions of Eq. (25)] for the modulational instability of CPEM waves that are scattered off electron density perturbations are shown for the same set of parameters as in Fig. 1 (a), but with $A_0 = 1.1$ for the dash-dotted lines.

III. DERIVATIONS AND ANALYSES OF NONLINEAR DISPERSION RELATIONS

To investigate the characteristics of SRS, SBS and MIs of a constant amplitude pump that is scattered off electron and ion plasma modes, and a spectrum of nonresonant electron and ion density perturbations, we express the vector potential \mathbf{A}_\perp as

$$\begin{aligned} \mathbf{A}_\perp = & \mathbf{A}_0 \exp(ik_0x - i\omega_0t) + c.c. \\ & + \sum_{+,-} \mathbf{A}_\pm \exp(ik_\pm x - i\omega_\pm t), \end{aligned} \quad (18)$$

where *c.c.* denotes the complex conjugate. The subscripts 0 and \pm stand for the CPEM pump and CPEM

sidebands, respectively, and $\omega_\pm = \Omega \pm \omega_0$, $k_\pm = k \pm k_0$ are the frequencies and wave numbers of the CPEM sidebands that are generated due to the interactions of the pump wave (ω_0, k_0) with preexisted low-frequency electrostatic plasma oscillations (Ω, K). Substituting Eq. (18) into the coupled sets of equations [(15), (16)] and [(15), (17)], we successively obtain the nonlinear dispersion relations for SRS and SBS of CPEM waves:

$$S_R = \frac{K^2}{\gamma_{e0}^3} \sum_{+,-} \frac{1}{D_\pm} |\mathbf{A}_0|^2, \quad (19)$$

and

$$S_B = \frac{\beta K^2}{\gamma_{e0}} \sum_{+,-} \frac{1}{D_\pm} |\mathbf{A}_0|^2, \quad (20)$$

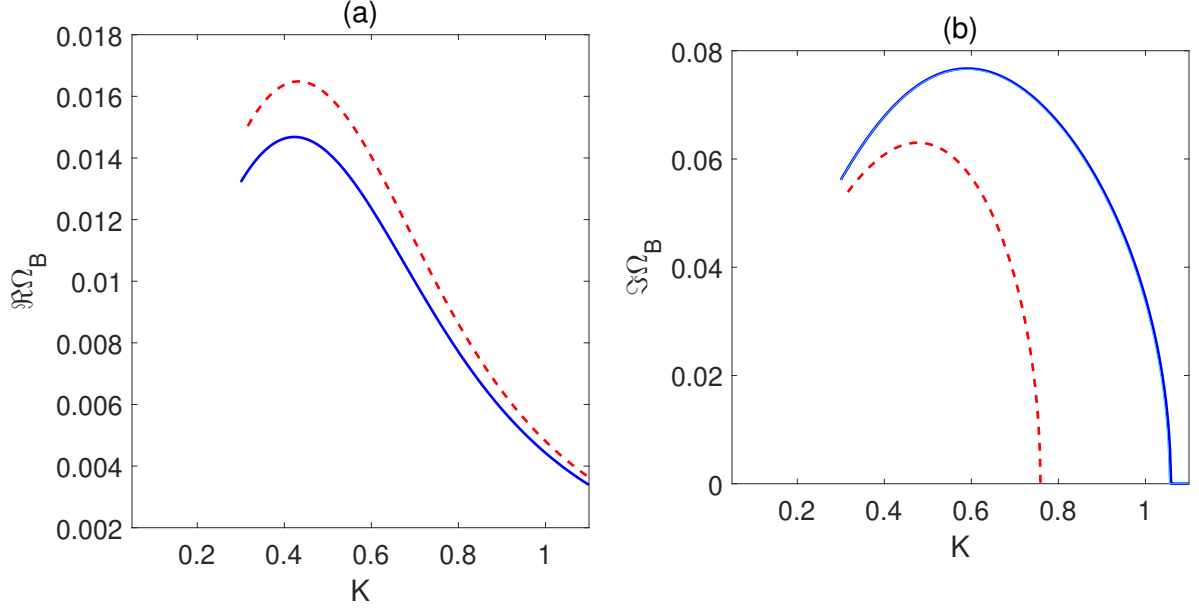


FIG. 3. The frequency shift ($\Re\Omega$) and the growth rate of instability ($\Im\Omega$) [numerical solutions of Eq. (26)] for the modulational instability of CPEM waves that are scattered off ion density perturbations are shown for the same set of parameters (for the solid and dashed lines) as in Fig. 1 (b).

where $S_R \equiv \Omega^2 - \sigma_e K^2 - 1/\gamma_{e0}$, $S_B \equiv \Omega^2 - K^2(m\sigma_e + \sigma_i)/\gamma_{i0}$, $D_{\pm} = \omega_{\pm}^2 - k_{\pm}^2 - 1 \approx \pm 2\omega_0(\Omega - K v_g \mp \delta)$ with $v_g = k_0/\omega_0$ denoting the dimensionless group velocity of the CPEM pump, $\omega_0 = \sqrt{1 + k_0^2}$ is the pump frequency, and $\delta = K^2/2\omega_0$ is the dimensionless nonlinear frequency shift. The dispersion relations (19) and (20) have the forms similar to those obtained in Ref. 2. In the latter, the authors investigated the stimulated scattering instabilities in nonrelativistic quantum plasmas with the effects of particle dispersion and exchange-correlation. The solutions of Eqs. (19) and (20), in fact, represent forward and backward SRS and SBS.

In the absence of the pump, $\gamma_{e0} = \gamma_{i0} = 1$ and $S_R = S_B = 0$, and we have the following dispersion relations for electron (Langmuir) and ion plasma oscillations.

$$\Omega_L = \sqrt{1 + \sigma_e K^2}, \quad \Omega_I = \sqrt{m\sigma_e + \sigma_i}K, \quad (21)$$

Next, we obtain the growth rates of instabilities for SRS and SBS instabilities, as well as for the MI of a pump of constant amplitude that is scattered off electron and ion plasma waves. For three-wave decay interactions, the maximum growth rates can be obtained when the scattered wave is also resonant, i.e., $D_- = 0$ ($\Omega = \Omega_L$) which gives

$$\omega_0 = (1 + \sigma_e K^2)^{1/2} + [1 + (K - k_0)^2]^{1/2}. \quad (22)$$

Thus, in an underdense plasma with $\omega_0 > 2$, one can show using Eq. (22) that the wave number K of resonant modes lies in $0 < K < 2k_0$. The modes with $K < k_0$ and $K > k_0$, respectively, correspond to forward and backward SRS/SBS instabilities. Neglecting the nonresonant terms ($\sim 1/D_+$) from Eqs. (19) and (20), and

letting $\Omega = (K v_g - \delta) + i\gamma_{R,B} = \Omega_{R,B} + i\gamma_{R,B}$, we obtain the growth rates for Raman and Brillouin backscattering ($K \simeq 2k_0 > k_0$) instabilities:

$$\gamma_R = \frac{k_0}{\sqrt{\omega_0 \Omega_R}} \frac{|\mathbf{A}_0|}{\gamma_{e0}^{3/2}}, \quad \gamma_B = \frac{k_0 \sqrt{\beta}}{\sqrt{\omega_0 \Omega_B \gamma_{e0}}} |\mathbf{A}_0|, \quad (23)$$

where $\Omega_{R,B} = \Omega_{L,I}$ at $K \simeq 2k_0$, i.e., $\Omega_R = \sqrt{1 + 4\sigma_e k_0^2}$ and $\Omega_B = 2k_0 \sqrt{m\sigma_e + \sigma_i}$. Though, the expressions for the growth rates, given by Eq. (23), are similar to those obtained in Ref. 2, however, the explicit dependencies of γ_R and γ_B on the CPEM pump wave amplitude A_0 are quite different due to the relativistic effects (γ_{e0} and γ_{i0}). Furthermore, the expressions of γ_R and γ_B are significantly modified by the relativistic degenerate pressure ($\propto \sigma_e$) of electrons and adiabatic thermal pressure ($\propto \sigma_i$) of ions. In particular, for large amplitude CPEM pump with $A_0 \gg 1$, Eq. (23) reduces to

$$\gamma_R \approx \frac{k_0}{\sqrt{\omega_0 \Omega_R}} |\mathbf{A}_0|^{-1/2}, \quad \gamma_B \approx \sqrt{\frac{m}{\omega_0 \Omega_B}} \frac{\sqrt{|\mathbf{A}_0|} k_0}{(1 + m^2 |\mathbf{A}_0|^2)^{1/4}}. \quad (24)$$

In this case, the terms proportional to the mass ratio m may no longer be negligible compared to the unity, and thus the relativistic effects of ions contribute to the development of SRS and SBS instabilities in the field of strong EM wave radiation.

Next, for the modulational instabilities of CPEM waves associated with the nonresonant electron and ion density perturbations, we retain both $D_{\pm} (\neq 0)$ and $S_{R,B} (\neq 0)$ in Eqs. (19) and (20). Thus, we obtain

$$S_R \left[(\Omega - K v_g)^2 - \delta^2 \right] = \frac{\delta K^2}{\omega_0 \gamma_{e0}^3} |\mathbf{A}_0|^2, \quad (25)$$

and

$$S_B \left[(\Omega - K v_g)^2 - \delta^2 \right] = \frac{\beta \delta K^2}{\omega_0 \gamma_{e0}} |\mathbf{A}_0|^2. \quad (26)$$

Equations (25) and (26) can be solved numerically to ascertain the growth rates of MIs of CPEM waves that are scattered by the nonresonant electron and ion density perturbations, which we will perform in Sec. IV.

IV. RESULTS AND DISCUSSION

We analyze numerically the characteristics of the growth rates for SRS and SBS instabilities given by Eq. (23). The results are displayed in Fig. 1. From the subplot 1 (a), it is seen that as one goes from weakly to strong relativistic degenerate plasmas (by increasing the number density and so increasing values of both R and σ), the growth rate for SRS instability γ_R is reduced (see the solid, dashed and dotted lines). Similar reduction is also possible with increasing values of the pump wave amplitude $A_0 > 1$ (compare the solid line with the dash-dotted line). This is in contrast to nonrelativistic plasmas [2] where $\gamma_{R,B} \propto |\mathbf{A}_0|$. Thus, it follows that even in the field of strong EM wave radiation, the growth rate of instability is enhanced in the regimes of weakly relativistic degenerate plasmas. On the other hand, subplot 1 (b) shows that the influence of the degenerate pressure of electrons is not so pronounced (as the corresponding terms are $\propto m$) unless the pump wave amplitude or the degeneracy parameter σ_e is sufficiently increased. As the ion thermal energy increases, the growth rate of SBS instability decreases. Similar to the SRS instability, we also find that the growth rate of SBS instability decreases with decreasing values of the pump wave amplitude A_0 .

Next, we numerically solve Eqs. (25) and (26) to obtain the frequency shifts ($\Re\Omega$) and the growth rates ($\Im\Omega$) of instabilities of the CPEM wave envelope of constant amplitude that is scattered off and modulated by the nonresonant electron and ion density perturbations. The corresponding results are exhibited in Figs. 2 and 3 respectively. From Fig. 2 we notice that the frequency of modulation is always up shifted and it increases as one goes from weakly relativistic to strong or ultra-relativistic regimes of degenerate electrons with increasing the number density. The frequency can, however, be higher even with lower values of the pump wave amplitude A_0 [see Fig. 2 (a)]. On the other hand, subplot Fig. 2 (b) shows that higher the concentration of number density (strong relativistic degenerate), lower is the growth rate of instability with cut-offs at lower wave numbers of modulation K (see the dotted line). Furthermore, the growth rate can be reduced by lowering the pump wave amplitude (see the dash-dotted line) as similar to nonrelativistic

plasmas. Figure 3 shows that the thermal pressure of ions significantly modify the frequency shift and the growth rate of instability of CPEM waves under the modulation of ion density perturbations. We find that while the values of ($\Re\Omega$) increase, those of ($\Im\Omega$) decrease with increasing values of the ion thermal energy.

V. CONCLUSION

We have investigated the nonlinear interactions of large amplitude high-frequency CPEM waves with low-frequency electrostatic electron and ion density perturbations that are driven by the CPEM ponderomotive force in an unmagnetized relativistic plasma with degenerate electrons and thermal ions. At the time scale of electron plasma period when ions do not respond, it is shown that the Langmuir wave spectra is significantly modified by the relativistic degenerate electrons, and are excited by the CPEM waves due to stimulated Raman scattering instability. In contrast to nonrelativistic plasmas, the growth rate of instability is shown to be reduced at higher values of the amplitude of the CPEM pump, and it is enhanced in strong relativistic degenerate plasmas. Furthermore, the inclusion of ion dynamics provides also the possibility of low-frequency ion-acoustic waves that are modified by the ion thermal pressure and are excited by the CPEM wave due to Brillouin scattering instability. In this case, the instability growth rate is seen to be enhanced at higher values of the amplitude of the CPEM pump or lower values of the ion thermal energy. We have also shown the possibility of the modulational instability of CPEM waves due to nonresonant electron and ion density perturbations. The characteristics of the frequency shifts and the growth rates of modulational instability are found to be distinctive from those in nonrelativistic regimes [2].

To conclude, the results of stimulated Raman and Brillouin scattering instabilities, as well as the modulational instability of ultra intense CPEM waves in a relativistic degenerate plasma is highly pertinent to understanding the salient features of enhanced density fluctuations and the dynamics of X -ray pulses that may emanate from compact astrophysical objects. The results can also be useful in the next-generation highly intense laser produced solid density compressed plasma experiments.

ACKNOWLEDGMENTS

This work was supported by UGC-SAP (DRS, Phase III) with Sanction order No. F.510/3/DRS-III/2015(SAPI), and UGC-MRP with F. No. 43-539/2014 (SR) and FD Diary No. 3668.

[1] G. T. Chanturia, V. I. Berezhiani, and S. M. Mahajan, Phys. Plasmas **24**, 074501 (2017).

[2] P. K. Shukla, B. Eliasson, and L. Stenflo, Phys. Rev. E

- 86**, 016403 (2012).
- [3] A. Singh and K. Balia, *Optik* **124**, 3470 (2013).
- [4] M. Salimullah and M. H. A. Hassan, *Phys. Rev. A* **41**, 6963 (1990).
- [5] K. M. Jain, M. Bose, and S. Guha, *Plasma Phys, Control Fusion* **26**, 677 (1984).
- [6] H. A. Rose, D. F. DuBois, and B. Bezzerides, *Phys. Rev. Lett.* **58**, 2547 (1987).
- [7] C. S. Liu and V. K. Tripathi, *Phys. Plasmas* **3**, 3410 (1996).
- [8] C. J. Walsh, D. M. Villeneuve, and H. A. Baldis, *Phys. Rev. Lett.* **53**, 1445 (1984).
- [9] D. N. Gupta, Pinki Yadav, D. G. Jang, M. S. Hur, H. Suk, and K. Avinash, *Phys. Plasmas* **22**, 052101 (2015).
- [10] J. Parashar, *Phys. Plasmas* **20**, 122101 (2013).
- [11] W. L. Kruer, *The Physics of Laser Plasma Interactions* (Addison-Wesley, Redwood City, CA, 1973).
- [12] S. H. Glenzer and R. Redmer, *Rev. Mod. Phys.* **81**, 1625 (2009).
- [13] M. C. Begelman, R. D. Blandford, and M. D. Rees, *Rev. Mod. Phys.* **56**, 255 (1984).
- [14] P. K. Shukla and B. Eliasson, *Phys. Rev. Lett.* **99**, 096401 (2007).
- [15] V. V. Zheleznyakov, *Radiation in Astrophysical Plasmas* (Kluwer Academic Publishers, 1996).
- [16] S. L. Shapiro and S. A. Teukolsky, *Black Holes, White Dwarfs, and Neutron Stars: The Physics of Compact Objects* (Wiley-VCH, Weinheim, 2004).
- [17] A. P. Misra and A. Roy Chowdhury, *Chaos, Solitons and Fractals* **15**, 801 (2003).
- [18] S. Chandrasekhar, *Mon. Not. R. Astron. Soc.* **95**, 207 (1935).
- [19] D. Verma, A. Das, P. Kaw, and S. K. Tiwari, *Phys. Plasmas* **22**, 013101 (2015).
- [20] S. Sundar, *Phys. Plasmas* **23**, 062104 (2016).